文章编号:1001-9014(2012)02-0106-07

Algorithm for eliminating stripe noise in infrared image

SUI Xiu-Bao, CHEN Qian, GU Guo-Hua

(National Defense Key Laboratory of Optoelectronic Engineering, Nanjing University of Science and Technology, Nanjing 210094, China)

Abstract: The mechanism of stripe noise was analyzed. An algorithm for eliminating stripe noise in one frame time was proposed. The algorithm obtains the extreme value of every row pixels by traversing all pixels of a frame in local window and computes noise gain and offset parameters through the succession of adjacent row pixels. By setting adaptive threshold value, eliminating the influences of image edges and system noise, we can achieve the precise gain and offset parameters and complete the eliminating algorithm for stripe noise. The experiment and theoretical analysis indicate that our algorithm can eliminate stripe noise effectively in one frame time.

Key words: infrared image; stripe noise; local window; threshold setting; succession

PACS: 42.30.-d

红外图像条纹噪声消除方法

隋修宝, 陈 钱, 顾国华

(南京理工大学 光电工程重点学科实验室,江苏 南京 210094)

摘要:分析了条纹噪声的产生机制,并提出了能够在一帧时间内完成的去除条纹噪声算法.该算法利用局部窗口遍历一帧图像的所有像元,获得每行像元的极值,并通过相邻行之间灰度值的继承性完成一帧图像的校正参数的计算;通过设定合适的阈值消除图像边缘和系统噪声对参数精度的影响.实验结果和理论分析表明,提出的算法能够在一帧时间内有效地消除红外图像的条纹噪声.

关 键 词:红外图像;条纹噪声;局部窗口;阈值设置;继承性

中图分类号:TN215 **文献标识码**:A

Introduction

Compared with visible images, infrared images generally have the shortcoming of low signal to noise ratio (SNR) which limits the application of infrared focal plane arrays (IRFPA). Fixed pattern noise (FPN), resulting from the channel difference of readout circuit and response difference of pixels, is a major part of infrared image noises. There are many correction algorithms for FPN [1-4]. These correction algorithms can be divided into two primary categories: 1) reference-based correction using calibrated images on startup; 2) scene based techniques continually recalibrating the sensor for parameter drifts. In addition to FPN, random noise is also a part of infrared images noises, while its energy is usually smaller than FPN. Random noise is composed of $1/f$ noise, thermal noise, biases voltage noise, etc. After some necessary non-uniformity correction algorithm, the energy of the FPN will be smaller and the random noise will be the major

Received date: 2011-04-25, **revised date**: 2011-12-11 **收稿日期**:2011-04-25, **修回日期**:2011-12-11

Foundation item: Supported by Jiangsu Natural Science Foundation (BK2011698); Specialized Research Fund for the Doctoral Program of Higher Education of China (20113219120017); China Postdoctoral Science Foundation (20110491424); Jiangsu Planned Projects for Postdoctoral Research Funds (1101081C)

Biography: SUI Xiu-Bao (1981-), male, Shandong Province, PhD. Research on electro-optical detecting and image engineering. Email: sxbhandsome@163.com.

noise. So, after the infrared images have been calibrated by the non-uniformity correction algorithm, they should continue to be processed to eliminate the random noise. Compared with FPN, the random noise has a feature that both of its amplitude and phase are usually different frame by frame. So, the eliminating algorithm for the random noise should be completed in one frame time (standard PLA, 40 ms). Among the random noise, stripe noise is a special kind of random noise. It is very obvious in row integration readout circuit, which is due to the working principle of the readout circuit.

Stripe noise is similar to non-uniformity in a frame time, but the usual non-uniformity correction algorithm is not adaptive to be used to eliminate stripe noise. The most typical reference-based correction methods are the so-called "one-point" correction method and the "two-point" correction method. Problems of the reference-based methods are that their parameters are fixed in a long time, while the stripe noise is variable frame by frame [5-6]. Scene based non-uniformity correction algorithm is developed to resolve the problems that the parameters of IRFPA drift slowly. However there are still two problems existing in scene based non-uniformity correction algorithm: 1) its convergence speed is slow: most algorithms need more than one frame time to complete convergence; 2) many algorithms are very complex and even can not meet the real-time demand. For these problems, the usual scene based non-uniformity correction algorithms are not adaptive to eliminate stripe noise [7-11]. However, there are some similarities between stripe noise and FPN. The parameters of gain and offset are computed like traditional non-uniformity correction algorithm in this paper except that they are computed in local window area to eliminate stripe noise in one frame time. In the algorithm we exclude the edge pixels of the image to eliminate their influence on parameter accuracy.

1　Sources of stripe noise

Stripe noise is very obvious in row integration readout circuit due to its working principle. Fig. 1 is the row integration readout circuit schematic of 320 × 240 uncooled microbolometer made in France. The working principles are as follows: 1) at one time t_1, the switch K_p is opened and K_c is closed. The readout circuit is at the reset state; 2) at time t_2, the switch K_p is closed and K_c is opened. The integration current i_p is controlled by the gate voltage V_{FID} of field-effect tube (FET). When the integration process completes, sampling capacitor samples the

last integration voltage and transports the value to the follow-up processing unit; 3) at time t_3, the switch K_p is opened and K_c is closed. The integration capacitor C_{int} is at the reset state. Repeated the process above, all row pixels can be picked up. According to the working principle of row integration readout circuit, it can be concluded that: the pixels in one row are biased by the bias voltage V_{FID} with the same noise voltage. When different rows integrate, the gate of FET will be biased by V_{FID} with different noise voltage, which results that even all the pixels expose in the same infrared radiation, the integration current i_p is different. Because of the randomness of bias voltage noise, the amplitude of stripe noise at different row is different. As a result the stripe in the infrared video rolls up and down.

The bias voltage V_{FID} amplifies the integration current i_p through FET, so the infrared image processed by non-uniformity correction algorithm can be expressed as

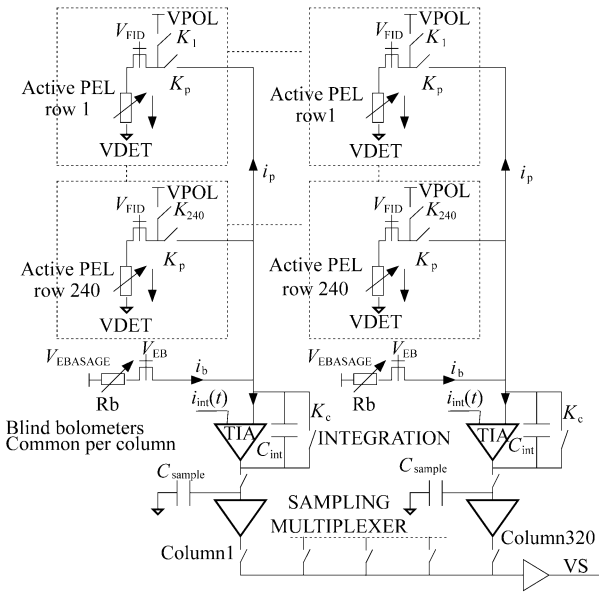

Fig. 1　Schematic of row integration readout circuit
图 1　行积分读出电路示意图

[12]:

$$V_{out} = aV + b \quad , \tag{1}$$

where, V is every FPA pixel's ideal output voltage; V_{out} is the output voltage when FET is biased by V_{FID}; a is the gain and b is the offset.

Each pixel of an image has its own response equation:

$$V_{out}(i,j) = a(i,j)V(i,j) + b(i,j) \quad , \tag{2}$$

where i is the row index and j the column index.

The readout circuit mentioned in Fig. 1 is analyzed now in the following equations. The infrared image has stripe noise and the parameters a and b of the same row pixels are the same respectively. Eq. (2) can be expressed as:

$$V_{out}(i,j) = a(i)V(i,j) + b(i) \quad , \tag{3}$$

where, $a(i)$ is the gain of row i; b_i is the offset of row i.

$V(i,j)$ is the ideal output. Eq. (2) is converted as:

$$\begin{aligned} V(i,j) &= (1/a(i))V_{out}(i,j) - b(i)/a(i) \\ &= \alpha(i)V_{out}(i,j) + \beta(i) \end{aligned} \quad , \tag{4}$$

where, $\alpha(i) = 1/a(i)$; $\beta(i) = -b(i)/a(i)$.

The linear transform of Eq. (4) can eliminate the stripe noise. Now the eliminating stripe noise method is translated into calculating the parameters $\alpha(i)$ and $\beta(i)$, and the calculation must be done in one frame time.

2 Algorithm descriptions

According to Eq. (4), in order to acquire parameters $\alpha(i)$ and $\beta(i)$, $V_{out}(i,j)$ and $V(i,j)$ should be get firstly. This is similar to solving parameters of "two point" non-uniformity correction algorithm. Because the parameters $\alpha(i)$ and $\beta(i)$ of Eq. (4) should be refreshed in every frame, so the "two point" non-uniformity correction algorithm is not ready to be used directly. In spite of this, we can use the solving parameter method for reference. If the edge pixels of an image have been excluded and the image does not have stripe noise, the pixel's voltage in the same column is almost the same. Based on the fact, we analyze a usual neural network non-uniformity correction method [13-16]. This method takes the average value of one pixel's four neighbors as the pixel's ideal output ($V(i,j)$). Referring to the method, we traversal every pixel in a row, then get the maximum and minimum pixels and compute the average value at the pixel's position (The average value is considered as the ideal output at the position). Following the steps above, $V_{out}(i,j)$ and $V(i,j)$ can be get, and then $\alpha(i)$ and $\beta(i)$ can be computed according to "two point" non-uniformity correction algorithm. During the process, if the images in row i and row $(i+1)$ are not all the edges and then we can get eligible maximum and minimum pixel value in row $(i+1)$, then, the images in row i and row $(i+1)$ have the succession. In order to reflect the succession, $\alpha(i+1)$ and $\beta(i+1)$ will be computed partly from $\alpha(i)$ and $\beta(i)$. The followings are a detailed description.

Our purpose is to eliminate stripe noise. However stripe may also be stripe object. To retain objects and at the same time eliminate stripe noise, we set a threshold ΔV. If the difference between one pixel voltage value and the mean of its neighborhood pixels is bigger than ΔV, it is thought that the pixel is at the edge of an image and should be excluded in the following statistics. In engineering, the value of ΔV is usually set to be larger than the maximal value of the stripe noise's line gradient to avoid treating stripe noise as image edges. Usually, the maximal value of the stripe noise does not change, so, the optimal value of ΔV can be fixed only once by experiments. Then the same ΔV can be always used in the same IR imager and will not cause problems. The equation about the nature of the pixels in an image should be calculated as:

$$v(i,j) = \begin{cases} 1, \text{when } abs(V(i,j) - V(i,j+1)) > \Delta V \text{ or} \\ \quad abs(V(i,j) - V(i+1,j)) > \Delta V, \text{else} \\ 0 \end{cases} \quad , \tag{5}$$

where, $abs()$ is absolute value function; if $v(i,j)$ equals to 1, the pixel at (i, j) (i is the row coordinate; j the column coordinate) is excluded in the following statistics.

Fig. 2 (a) is an infrared image with stripe noise; Fig. 2(b) is a binaryzation image after edge detection by Eq. (5). From Figs. 2 (a) and (b), it is found that Eq. (5) can exclude edge pixels but include the stripe noise pixels. So in the image processed by Eq.

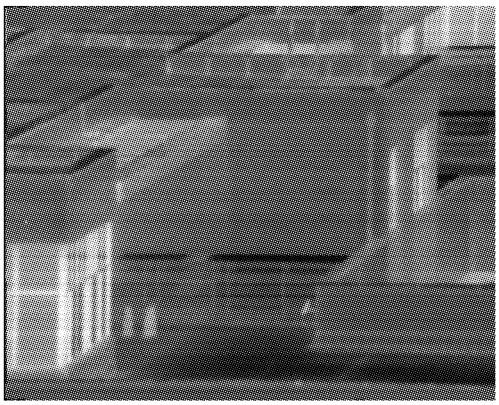

(a)

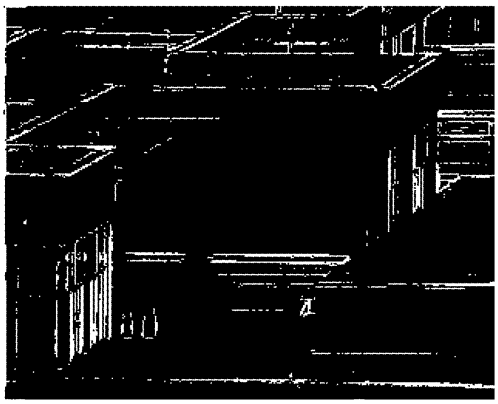

(b)

Fig. 2　(a) Image with stripe noise, (b) excluded pixels locations (white locations)
图 2　(a)含条纹噪声的红外图像,(b)不需计算的像元位置(白色位置)

(5), the value of adjacent pixel voltage varies slowly. We make a 1×2 window convolved with the infrared image with stripe noise. By using this method, the maximum and minimum value of every row pixels can be acquired. The extreme value is the mean of the two adjacent pixels at the same row. During the process of finding extreme value, if there are edge pixels according to Eq. (5) in the 1×2 window, the pixels can not be treated as extreme value. The equation is as follow:

$$\begin{cases} V_{\min}(i) = (V(i,j) + V(i,j+1))/2, \\ \quad \text{if } (V_{\min}(i) > (V(i,j) + (V(i,j+1))/2) \text{and } (v(i,j) = 0) \\ V_{\max}(i) = (V(i,j) + V(i,j+1))/2, \\ \quad \text{if } (V_{\max}(i) < (V(i,j) + (V(i,j+1))/2) \text{and } (v(i,j) = 0) \end{cases}, \quad (6)$$

where, $V_{\min}(i)$ is the minimum value of non-edge pixels at row i; $V_{\max}(i)$ is the maximum value of non-edge pixels at row i.

The positions of $V_{\min}(i)$ and $V_{\max}(i)$ are:

$$\begin{cases} \max(i) = j, \text{ when } V_{\max}(i) \text{ if updated} \\ \min(i) = j, \text{ when } V_{\min}(i) \text{ if updated} \end{cases}, \quad (7)$$

where, $(i, \max(i))$ is the position of $V_{\max}(i)$; $(i, \min(i))$ is the position of $V_{\min}(i)$.

Using Eq. (6) to traverse all non-edge pixels at a row (subscript j stands for the column index), then the maximum and minimum value of every row can be obtained. $V_{\min}(i)$, $V_{\max}(i)$ are similar to the response values of low temperature blackbody and high temperature blackbody separately in "two point" non-uniformity correction algorithm. For the purpose of decreasing signal noise's influence to $\alpha(i)$ and $\beta(i)$, the difference between $V_{\max}(i)$ and $V_{\min}(i)$ should be big enough. Then we set the threshold ΔV_m and define the following equation:

$$v''(i) = \begin{cases} 1 \text{ when } V_{\max}(i) - V_{\min}(i) > \Delta V_m \text{ else} \\ 0 \end{cases}, \quad (8)$$

where, the value 1 of $v''(i)$ indicates that there are $V_{\max}(i)$ and $V_{\min}(i)$ at row i which are used to compute the parameters $\alpha(i)$ and $\beta(i)$. The value 0 of $v''(i)$ indicates that there are no appropriate $V_{\max}(i)$ and $V_{\min}(i)$ to compute $\alpha(i)$ and $\beta(i)$. In other words, the value 0 of $v''(i)$ indicates that the pixels of i row and $(i+1)$ row are mostly the edge of image and the details of the images are abundant. The vision is sensitive to details of the images and the stripe noise at row i and row $(i+1)$ will not cause great stimulation to vision. So, $\alpha(i)$ is set as 1, $\beta(i)$ as 0, namely, the image at row i is kept unchanged.

When the value of $v''(i)$ is 1, there are three different situations as described in the following:

1: if $v''(i-1)$ is equal to 0 and $v''(i+1)$ equals to 0, there are abundant image edges at row $(i-1)$ and row $(i+1)$. Parameters $\alpha(i)$ and $\beta(i)$ can not be acquired from adjacent row pixels. $\alpha(i)$ and $\beta(i)$ are set as 1 and 0, respectively, namely, the pixels at i row are kept unchanged.

2: if $v''(i-1)$ is equal to 0 and $v''(i+1)$ is equal to 1, $\alpha(i)$ and $\beta(i)$ can not inherit from $\alpha(i-1)$ and $\beta(i-1)$. This time, according to neural network non-uniformity correction algorithm, the gray mean of $(i, \max(i))$ and $(i, \min(i))$'s four neighborhood pixels can be set as the real response of $(i, \max(i))$

and $(i, \min(i))$, respectively. Then, the parameters $\alpha(i)$ and $\beta(i)$ can be get. The equation is:

$$V_{\max ave}(i) = (V(i,\max(i)) + V(i,\max(i)+1) + V(i+1,\max(i)) + V(i+1,\max(i)+1))/4 \quad (9)$$

$$V_{\min ave}(i) = (V(i,\min(i)) + V(i,\min(i)+1) + V(i+1,\min(i)) + V(i+1,\min(i)+1))/4 \quad (10)$$

$$\alpha(i) = (V_{\max ave}(i) - V_{\min ave}(i))/(V_{\max}(i) - V_{\min}(i)) \quad (11)$$

$$\beta(i) = (V_{\max ave}(i) \times V_{\min}(i) - V_{\min ave}(i) \times V_{\max}(i))/(V_{\max(i)} - V_{\min}(i)) \quad (12)$$

where, $V_{\max ave}(i)$ is the estimation of true response at $(i, \max(i))$; $V_{\min ave}(i)$ is the estimation of true response at $(i, \min(i))$. This kind of estimation method is used widely in neural network non-uniformity correction algorithm.

From the typical Eqs. (11) and (12), we can get $\alpha(i)$ and $\beta(i)$.

3: when $v''(i-1)$ is equal to 1, in order to make sure that the gray difference of the pixels at row $(i-1)$ and row i, we make $\alpha(i)$ and $\beta(i)$ inherit from $\alpha(i-1)$ and $\beta(i-1)$. Eqs. (9) and (10) can be modified as:

$$V_{\max ave}(i) = \alpha(i-1) \times V_{\max}(i-1) + \beta(i-1) \quad (13)$$

$$V_{\min ave}(i) = \alpha(i-1) \times V_{\min}(i-1) + \beta(i-1) \quad (14)$$

Parameters $\alpha(i)$ and $\beta(i)$ are computed by Eqs. (11) and (12).

Finishing the steps above, we can acquire parameters $\alpha(i)$ and $\beta(i)$. According to the parameters, stripe noise will be eliminated in one frame time.

3 Experiments verification

A 320×240 pixel uncooled IRFPA imager operating in the wavelength range of approximately 8 ~ 14 μm is adopted to test our presented algorithm. The detector adopts the readout integrated circuit (ROIC) described in Fig. 1. The following images are all processed by NUC algorithm previously.

Fig. 3(a) shows an original infrared image. Fig. 3 (b) shows the infrared image with Gauss stripe noise. Its parameters are set as: $\mu = 0, \sigma = 4$. Fig. 4 (c) shows the image edges which are expressed by $v'(i,j)$ (listed in Eq. (5)). ΔV is set as three times of σ, assuring that the stripe noise is not be treated as image edges.

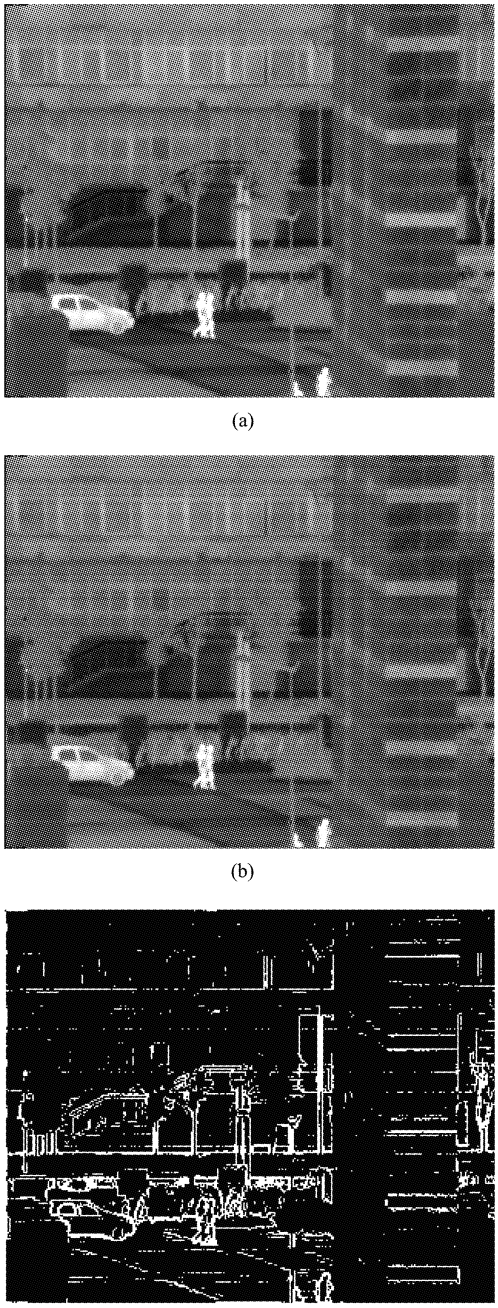

(a)

(b)

(c)

Fig. 3 (a) Original infrared image, (b) infrared image with Gauss stripe noise, (c) infrared image edges (white locations)
图3 (a)原始红外图像,(b)含高斯噪声的红外图像,(c)红外图像边缘(白色位置)

ΔV_m in Eq. (8) should be set according to the system noise of thermal imager. To our thermal imager, ΔV_m is 40 mV which is tested by CI thermal imager test system. The test condition is: the environment temperature is 300 K; F# of infrared lens is 1.0; focus length of infrared lens is 50 mm. In order to eliminate the influence to $\alpha(i)$ and $\beta(i)$.

Fig. 4　Image processed by the algorithm in this paper
图 4　经本文算法处理过后的红外图像

ΔV_m is set to be equal to 80 mV during the calculation (ΔV_m can be set bigger. However, if the value is too big, we may not get appropriate $V_{\max}(i)$, $V_{\min}(i)$. What's more, may not get $\alpha(i)$ and $\beta(i)$). Adopting the algorithm mentioned in the last section, we process Fig. 3 (b) and get Fig. 4.

Comparing Fig. 3 (b) with Fig. 4, it can be found that, the stripe noise amplitude in Fig. 4 is smaller than in Fig. 3 (b). Comparing with Fig. 3 (a), there is still some weak stripe noise in Fig. 4. The results indicate that the algorithm for eliminating stripe noise brought forward in this paper is efficient and it can eliminate most of the stripe noise in the infrared images.

In order to assess our algorithm objectively, mean-squared error (MSE) is adopted to analyze the performance of our algorithm. MSE is defined as [15]:

$$\mathrm{MSE}_{\mathrm{dn}} = \sum_{i=1}^{M}\sum_{j=1}^{N}(V_{\mathrm{o}}(i,j) - V_{\mathrm{dn}}(i,j)^2/(M \times N)) \quad , \quad (15)$$

$$\mathrm{MSE}_{\mathrm{da}} = \sum_{i=1}^{M}\sum_{j=1}^{N}(V_{\mathrm{o}}(i,j) - V_{\mathrm{da}}(i,j)^2/(M \times N)) \quad , \quad (16)$$

where $V_{\mathrm{o}}(i,j)$ is the pixel voltage without stripe noise. $V_{\mathrm{dn}}(i,j)$ is the pixel voltage with stripe noise. $V_{\mathrm{da}}(i,j)$ is the pixel voltage after our algorithm. M and N is row number and column number, respectively.

MSE is computed according to Fig. 3 (a), (b) and Fig. 4. The finally data are shown in Table 1.

Table 1　MSE of different images
表 1　不同图像的 MSE

MSE	$\mathrm{MSE}_{\mathrm{dn}}$	$\mathrm{MSE}_{\mathrm{da}}$
DATA	16	1.45

From Table 1, it can be found that $\mathrm{MSE}_{\mathrm{da}}$ is obviously smaller than $\mathrm{MSE}_{\mathrm{dn}}$. We change the amplitude of stripe noise in Fig. 3 (b) and get MSE in Table 2. From Table 2, it can be found that with σ increasing, $\mathrm{MSE}_{\mathrm{dn}}$ becomes larger and lager but $\mathrm{MSE}_{\mathrm{da}}$ changes a little. The experiment data indicates that our algorithm is effective in eliminating stripe noise which is consistent with the conclusion we made from subjective image comparison.

Table 2　MSE of different images with different σ
表 2　σ 不同时图像的 MSE

MSE	$\mathrm{MSE}_{\mathrm{dn}}$	$\mathrm{MSE}_{\mathrm{da}}$
$\sigma = 2$	4.1	1.3
$\sigma = 3$	9.2	1.43
$\sigma = 5$	24.8	1.8
$\sigma = 8$	59	2.1
$\sigma = 10$	92.1	2.2

The last problem is that whether our algorithm can be completed in one frame time. We simulate the program in Matlab R2008a. In the program, the algorithm can be completed in the time of traversing all pixels three times. The three times traversing process is that: 1) accruing the edges pixel; 2) the maximum and minimum pixels' statistics of non-edge pixies; 3) the gain and offset of each pixel. If we process a 320 × 240 pixels' image and utilize dm642 (which is made in TI Corporation and the its master clock can be up to 600 MHz) as main processor, and assume that every instruction cost six clock periods (most instructions cost less than six clock periods[16]), the time our algorithm need is:

$$t = 320 \times 240 \times \left(\frac{1}{600}\mu s\right) \times 6 \times 3 = 2.304 \text{ ms} \quad , \quad (17)$$

which is much less than a frame time and the algorithm brought forward in this paper is real-time.

4　Conclusions

In this study, an eliminating stripe method for infrared images is proposed. This algorithm computes the parameters of gain and offset in local window and takes use of the succession of adjacent rows. In the processing, according to the SNR of adopted thermal imager, adaptive threshold ΔV and ΔV_m are selected to eliminate the influence of image edges and random noise.

The experiment results and theoretical analysis indicate that our algorithm can eliminate stripe noise effectively and also can be completed in one frame time.

REFERENCES

[1] Ni C, Li Q, Xia L Z. A novel method of infrared image denoising and edge enhancement [J]. *Signal Processing*, 2008, **88**(6): 1606 - 1614.

[2] Vergara L, Bernabeu P. Automatic signal detection applied to fire control by infrared digital signal processing[J]. *Signal Processing*, 2000, **80**(4): 659 - 669.

[3] Hardie R C, Baxley F, Brys B, *et al.* Scene-based nonuniformity correction with reduced ghosting using a gated LMS algorithm [J]. *Optics Express*, 2009, **17** (17): 14918 - 14933.

[4] Leathers R, Downes T, Priest R. Scene-based nonuniformity corrections for optical and SWIR pushbroom sensors[J]. *Optics Express*, 2005, **13**(13): 5136 - 5150.

[5] Hardie R C, Hayat M M, Armstrong E Y, *et al.* Scene-based nonuniformity correction with video sequences and registration[J]. *Applied Optics*, 2000, **39**(8): 1241 - 1250.

[6] Narayanan B, Hardie R C, Muse R A. Scend-based nonuniformity correction technique that exploits knowledge of the focal-plane array readout architecture[J]. *Applied Optics*, 2005, **44**(17): 3482 - 3491.

[7] Harris J G, Chiang Y M. Nonuniformity correction of infrared image sequences using the constant-statistics constraint [J]. *IEEE Trans. Image Processing*, *IEEE Transactions on*, 1999, **8**(8): 1148 - 1151.

[8] Kim J H, Ahn S S, Kwon C H, *et al.* An output channel nonuniformity compensation driving method in flat panel display driving circuits[J]. *Display Technology*, 2006, **2**(4): 386 - 392.

[9] Cohen M, Cauwenberghs G. Floating-gate adaptation for focal-plane online nonuniformity correction[J]. *Circuits and Systems II: Analog and Digital Signal Processing*, *IEEE Transactions on*, 2001, **48**(1): 83 - 90.

[10] Hatle M, Vobecky J. Infrared observation of gate turn-off thyristor segment parameter nonuniformity [J]. *Electron Devices*, *IEEE Transactions on*, 1990, **37**(4): 1169 - 1171.

[11] Tabib-Azar M, Pathak P S, Ponchak G, *et al.* Nondestructive superresolution imaging of defects and nonuniformities in metals, semiconductors, dielectrics, composites, and plants using evanescent microwaves[J]. *Review of Scientific Instruments*, 1999, **70**(6): 2783 - 2792.

[12] Sui X B, Chen Q, Gu G H, *et al.* Research on the response model of microbolometer [J]. *Chin. Phys. B*, 2010, **19**(10): 108702-1-10.

[13] Wang B J, Liu S Q, Bai L P. An enhanced non-uniformity correction algorithm for IRFPA based on neural networkwork[J]. *Optics Communications*, 2008, **281** (8): 2040 - 2045.

[14] Wang B J, Liu S Q, Lai R. Adaptive non-uniformity correction algorithm for IRFPA based on neural networkwork [J]. *J. Infrared Milim Waves*, 2006, **25**(6): 405 - 407.

[15] Przelaskowski A, Jóźwiak R, Krzyżewski T, *et al.* Ordering of diagnostic information in encoded medical images [J]. *Accuracy progression*, *Image Processing Technology*, 2008, **16**(1): 49 - 59.

[16] SM320DM642-EP Video/imaging fixed point digital signal processor. USA: Ti corporation (2007).

(上接101页)

REFERENCES

[1] Zhu J X, Balatsky A V. Josephson current in the presence of a precessing spin [J]. *Phys. Rev. B*, 2003, **67** (17): 174505.

[2] Sun Q F, Zhu Y, Lin T H. Writing spin in a quantum dot with ferromagnetic and superconducting electrodes [J]. *Phys. Rev. B*, 2004, **69**(12): 121302.

[3] Kobayashi K, Aikawa H, Katsumoto S, *et al.* Tuning of the Fano effect through a quantum dot in an Aharonov-Bohm interferometer[J]. *Phys. Rev. Lett.*, 2002, **88**(25): 256806.

[4] Domanski T, Donabidowicz A, Wysokinski K I. Meservey-Tedrow-Fulde effect in a quantum dot embedded between metallic and superconducting electrodes [J]. *Phys. Rev. B*, 2008, **78**(14): 144515.

[5] Stefanski P. Proposal for a correlation induced spin-current polarizer[J]. *Phys. Rev. B*, 2008, **77**(12): 125331.

[6] Sergueev N, Sun Q F, Guo H, *et al.* Spin-polarized transport through a quantum dot: Anderson model with on-site Coulomb repulsion [J]. *Phys. Rev. B*, 2002, **65** (16): 165303.

[7] Ma J, Dong B, Lei X L. Quantum transport through double-dot Aharonov-Bohm interferometry in Coulomb blockade regime[J]. *Eur. Phys. J. B*, 2003, **36**(4): 599 - 605.

[8] Dong B, Djuric I, Cui H L, *et al.* Time-dependent resonant tunneling for parallel-coupled double quantum dots[J]. *J. Phys. Condens. Matter*, 2004, **16**(24): 4303 - 4314.

[9] Dong B, Lei X L, Horing N J M. First-order coherent resonant tunneling through an interacting coupled-quantum-dot interferometer: Generic quantum rate equations and current noise[J]. *Phys. Rev. B*, 2008, **77**(8): 085309.

[10] Chi F, Zheng J, Sun L L. Spin accumulation and pure spin current in a three-terminal quantum dot ring with Rashba spin-orbit effect[J]. *J. Appl. Phys.*, 2008, **104** (4): 043707.

[11] Ying Y B, Jin G J, Ma Y Q. Spin-polarized transport through an Aharonov-Bohm interferometer embedded with a quantum dot molecule [J]. *J. Phys. Condens. Matter*, 2009, **21**(27): 275801.